Electronic Supplementary Material (ESI) for Journal of Materials Chemistry B.

Supporting Information

Particle Attachment Crystallization Facilitates the Occlusion of Micrometer-sized *Escherichia Coli* in Calcium Carbonate Crystals with Stable Fluorescence

Mengqi Zhang,[a†] Hang Ping,[a†] Weijian Fang,[a] Fuqiang Wan,[a] Hao Xie,[b] Zhaoyong Zou*[a] and Zhengyi Fu*[a]

a State Key Laboratory of Advanced Technology for Materials Synthesis and Processing, Wuhan University of Technology, Wuhan, 430070, China.

b School of Chemistry, Chemical Engineering, and Life Science, Wuhan University of Technology, Wuhan, 430070, China.

† These authors contributed equally.

* Corresponding authors, E-mail: zyfu@whut.edu.cn; zzou@whut.edu.cn

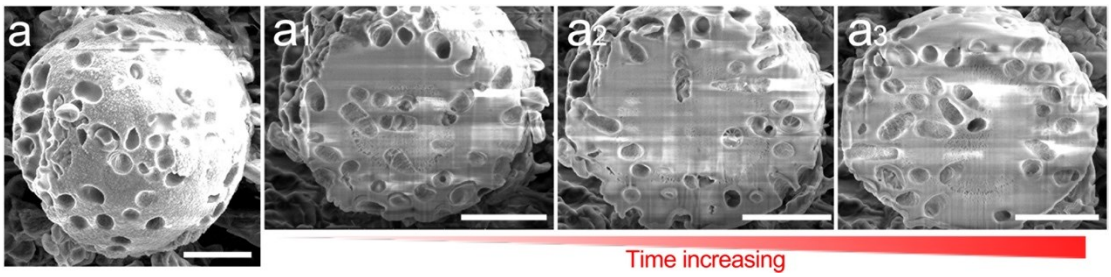

Figure S1. (a) Focused ion beam (FIB) etching of a single *E. coli*/vaterite crystal. Scale bar is 2 μm in a, 2.5 μm in a1-a3.

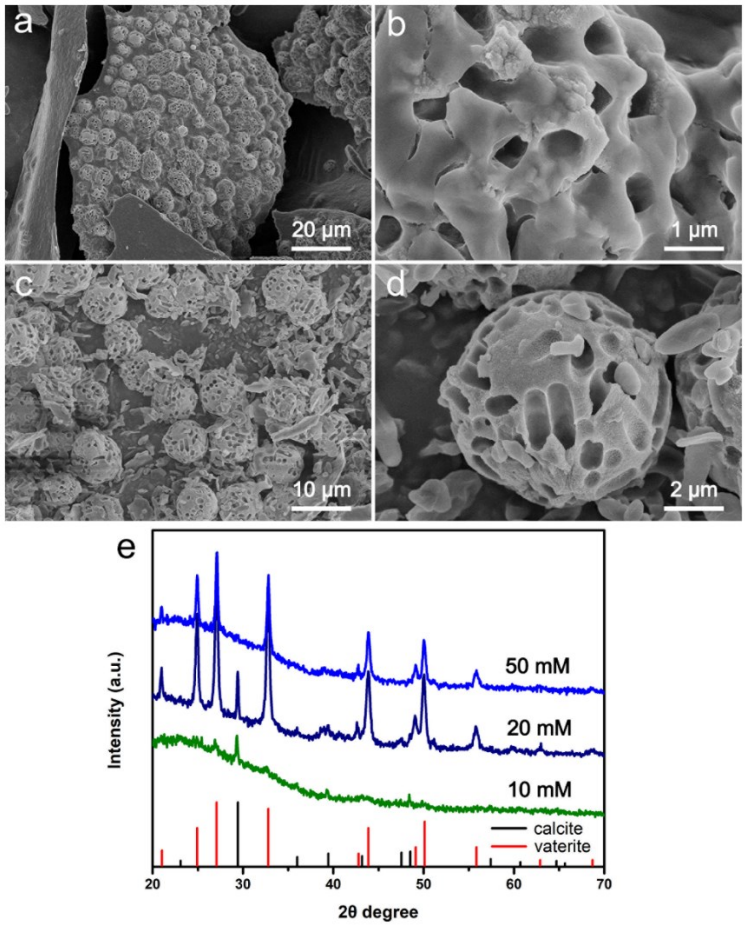

Figure S2. SEM images of composites under the concentration of (a-b) 10 mM and (c-d) 20 mM. (e) XRD patterns of composites with different concentrations.

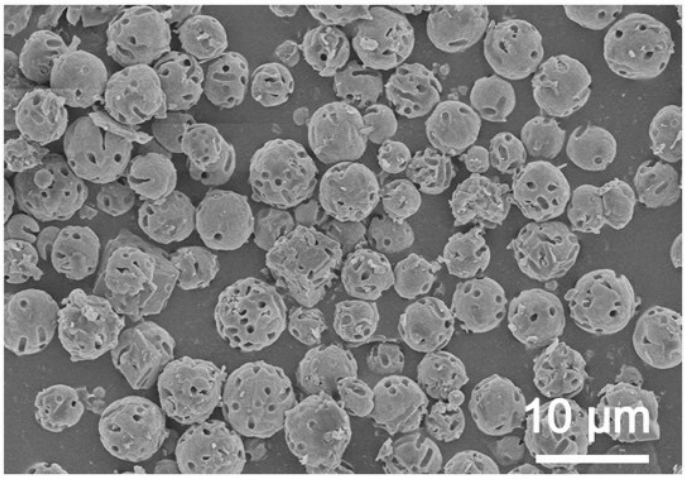

Figure S3. SEM image of *E. coli*/vaterite after mineralization for 10 min.

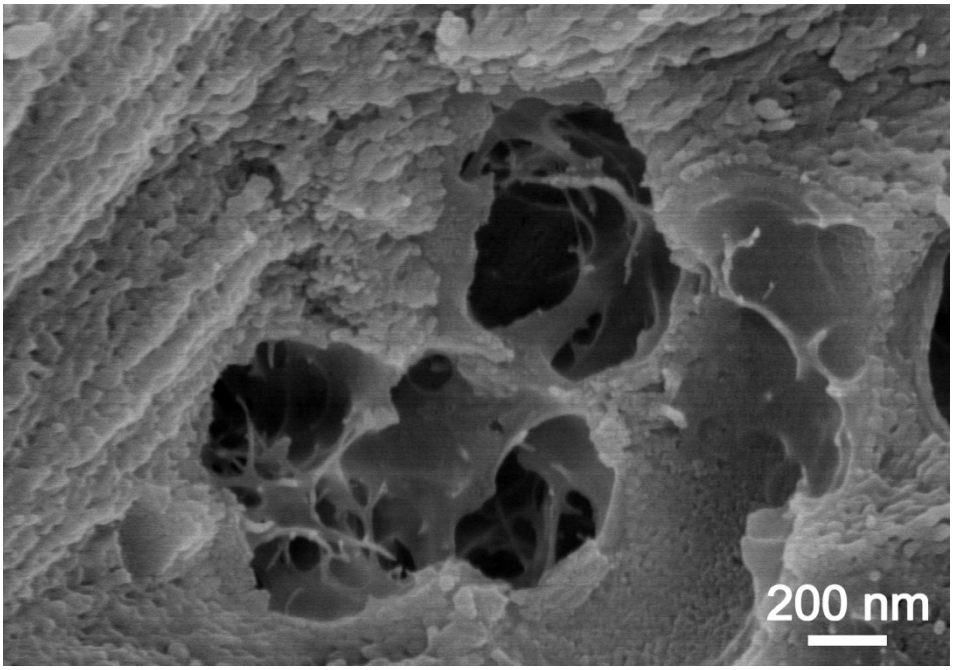

Figure S4. SEM image of fiber-like structure within the host crystal.

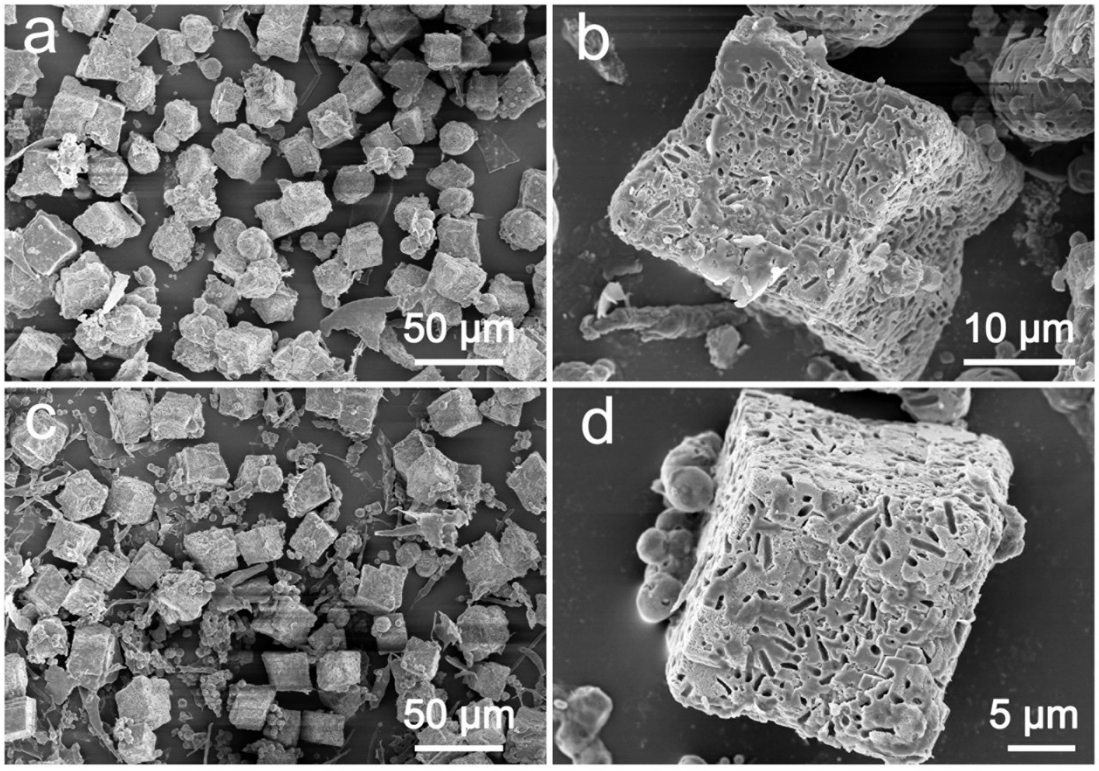

Figure S5. SEM images of *E. coli*/calcite composites after 5 min (a-b) and 10 min (c-d) of mineralization.

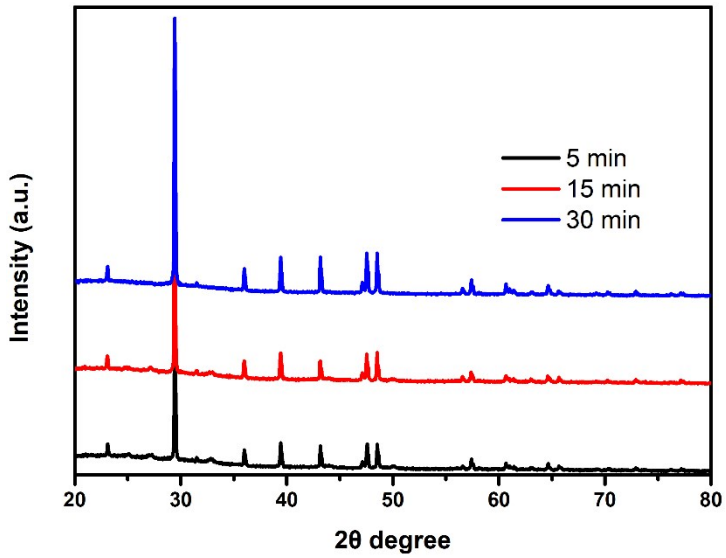

Figure S6. XRD patterns of *E. coli*/calcite composites.

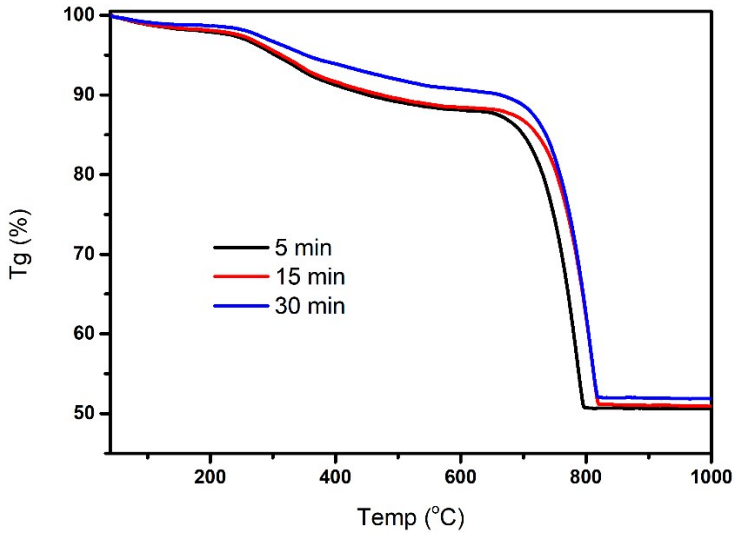

Figure S7. Thermogravimetric curves of *E. coli*/calcite composites.

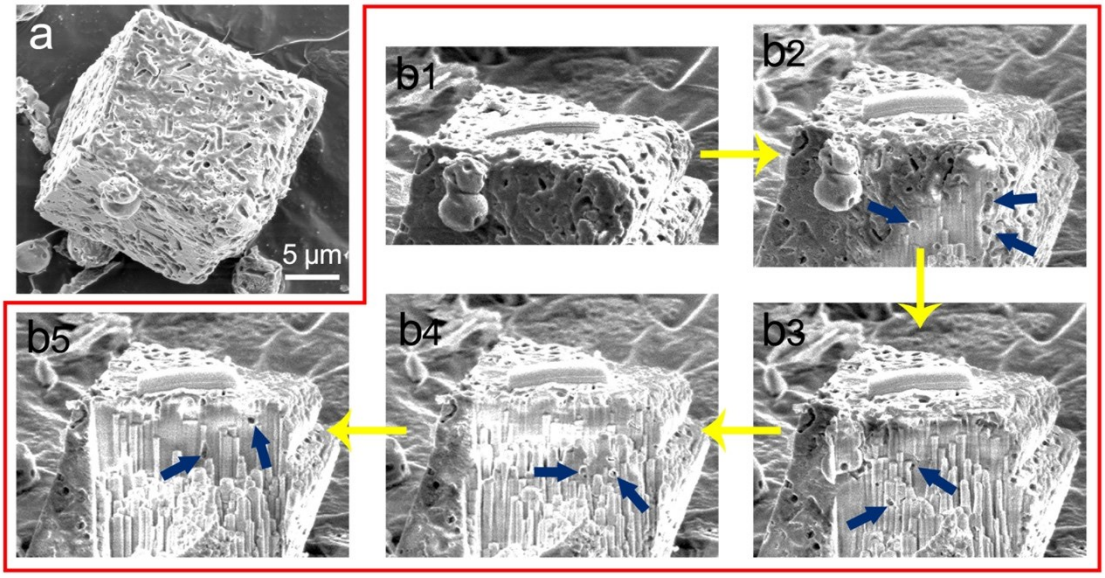

Figure S8. (a) SEM image of *E. coli*/calcite (top view). (b) Focused ion beam (FIB) etching of single calcite crystal (side view). The bacteria pores were marked by blue arrows.

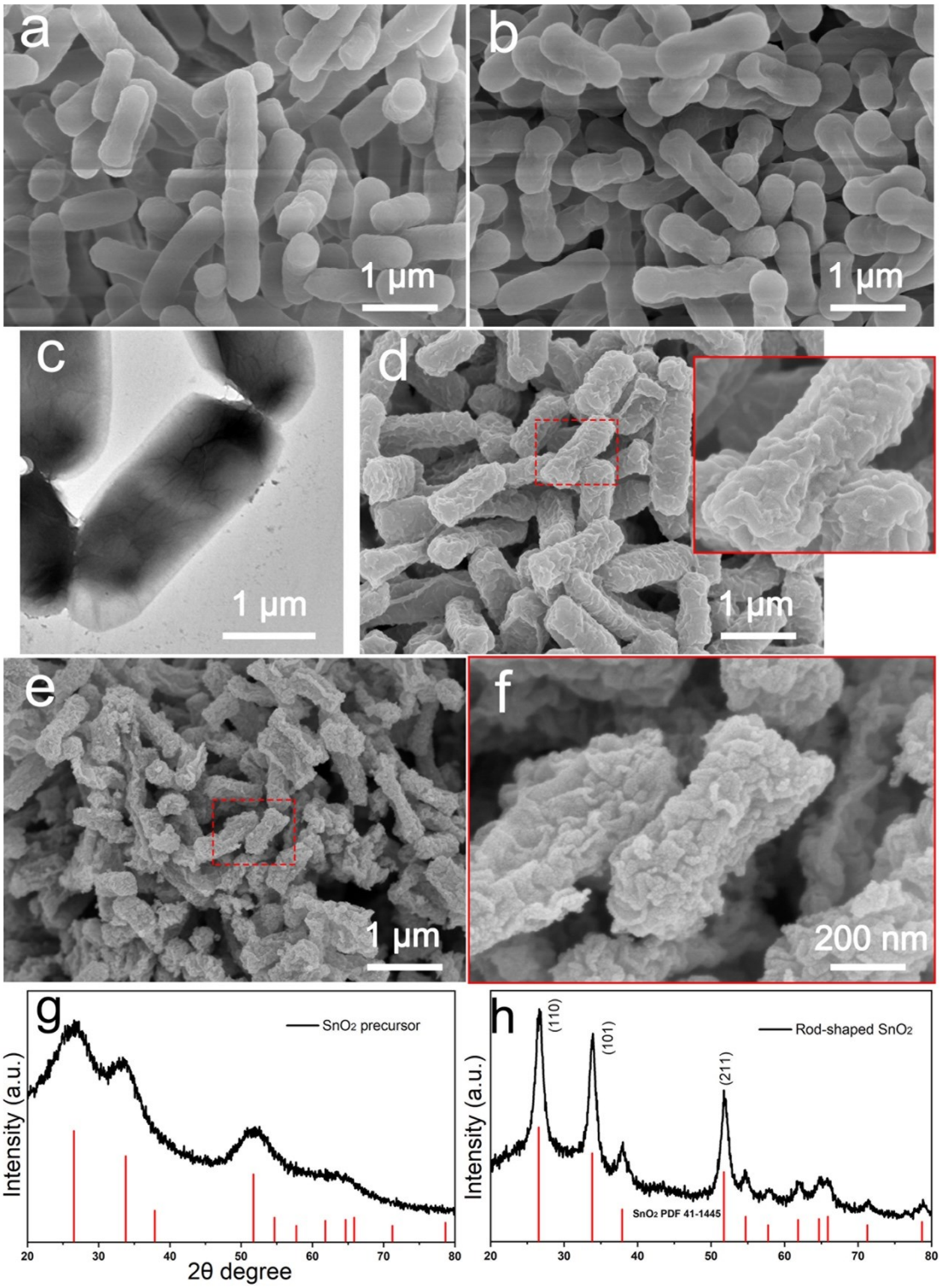

Figure S9. Morphology of various rod-shaped guest species with different surface structure and composition. (a) SEM image of native *E .coli*, (b) SEM image of 5R5 modified *E. coli*, (c) TEM image of *E. coli* with flagellum, (d) SEM image of SnO_2 precursor deposited *E. coli*. (e-f) SEM images of rod-shaped SnO_2. (g) XRD pattern of SnO_2 precursor, (h) XRD pattern of Rod-shaped SnO_2.

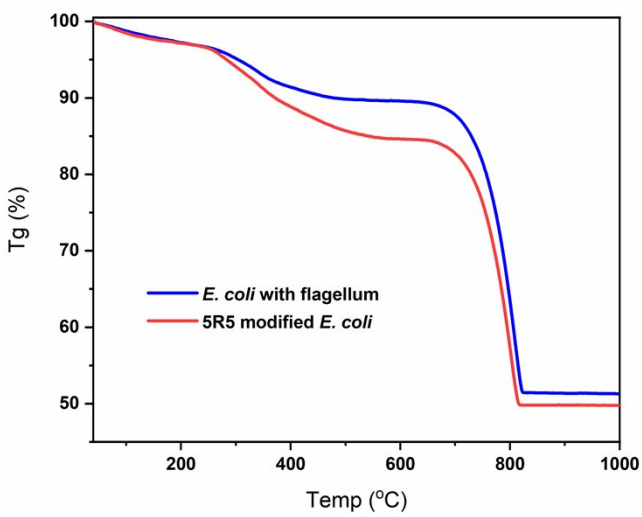

Figure S10. Thermogravimetric curves of guest/vaterite composites after 10 min of mineralization.

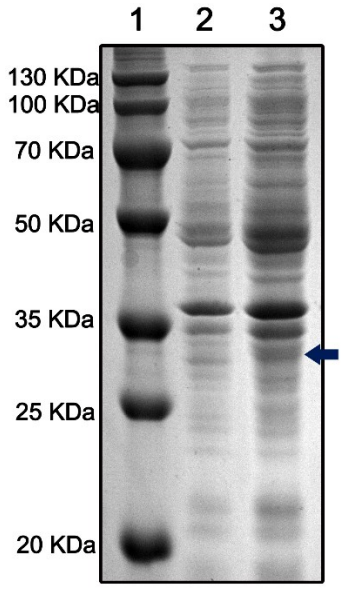

Figure S11. SDS-PAGE of GFP-modified *E. coli*. Lane 1, molecular weight marker; Lane 2, lysate of uninduced cells; Lane 3, lysate of IPTG-induced cells. The target band was marked by blue arrow.

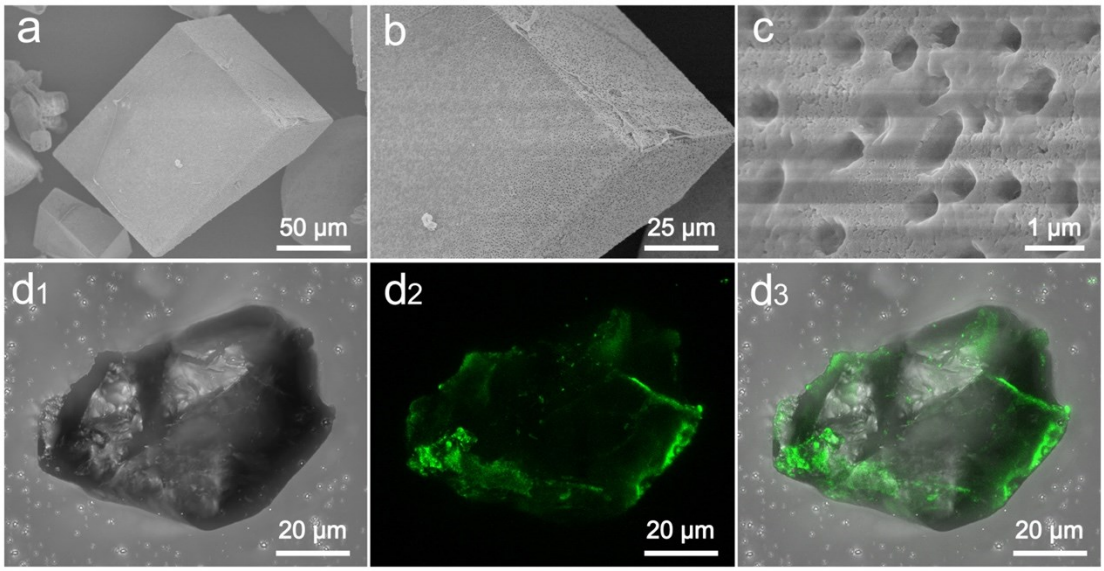

Figure S12. (a-c) SEM images of products synthesized by vapor diffusion method. (d1-d3) Confocal fluorescence images.

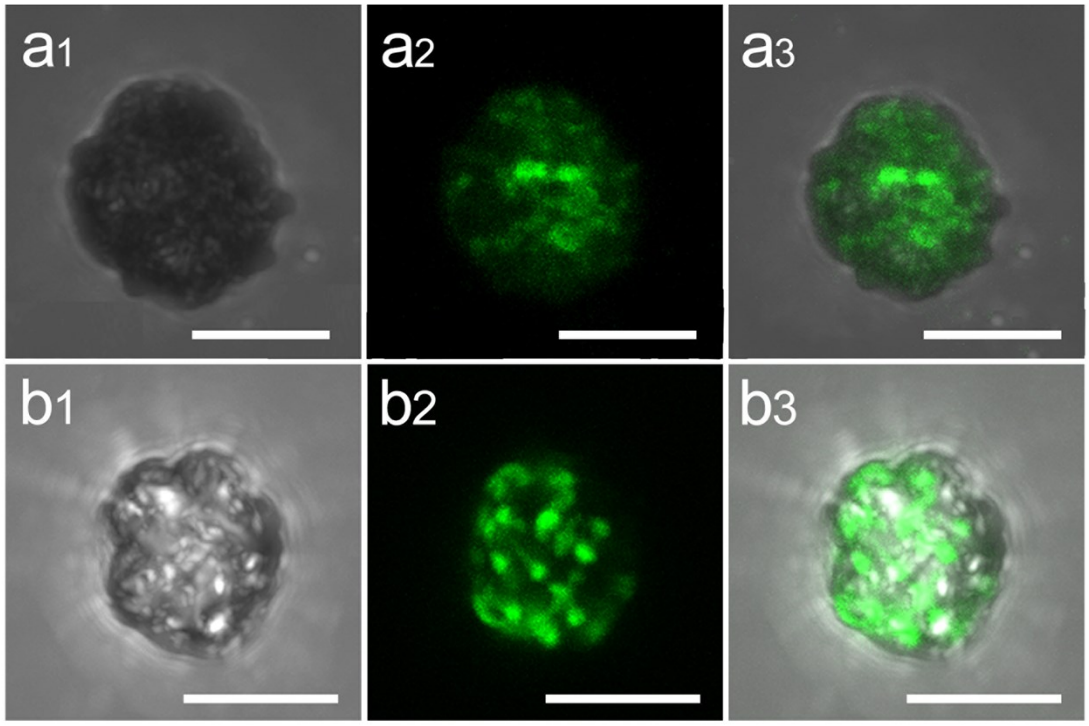

Figure S13. Confocal fluorescence images of GFP-*E. coli*/vaterite composite after (a) 3 months, (b) 6 months. Scale bar is 5 μm.

Table S1 FTIR data of *v*2 and *v*4 in *E. coli*/vaterite composites.

	*v*2 (876 cm^{-1})	*v*4 (745 cm^{-1})	*v*4 (713 cm^{-1})
Transmittance (%)	45.34	86.6	93.19
Absorbance	0.343	0.0625	0.0306

Table S2 The mass loss during different temperature region.

	40-200 °C	200-600 °C	600-1000 °C	Total loss
E. coli/ACC	18.2 %	12.9 %	28.8 %	59.9 %
E. coli/vaterite	3.8 %	16.0 %	34.0 %	53.8 %

Table S3. The multi-exponential lifetime (T_i) and preexponential (α_i) for lifetime of GFP-*E. coli*/$CaCO_3$ composites.

	α_1	T_1	α_2	T_2
GFP-*E. coli*/vaterite	3.435	1.222	0.0747	19.029
GFP-*E. coli*/calcite	3.630	1.479	0.0035	-0.0017